METHODS 19, 222–233 (1999)
Article ID meth.1999.0853, available online at http://www.idealibrary.com on IDEAL®

Quantification of Protein–Protein Interactions Using Fluorescence Polarization

David M. Jameson[1] and Steven E. Seifried

Department of Genetics and Molecular Biology, University of Hawaii, 1960 East–West Road, Honolulu, Hawaii 96822

Quantitative determinations of the dissociation constants of biomolecular interactions, in particular protein–protein interactions, are essential for a detailed understanding of the molecular basis of their specificities. Fluorescence spectroscopy is particularly well suited for such studies. This article highlights the theoretical and practical aspects of fluorescence polarization and its application to the study of protein–protein interactions. Consideration is given to the nature of the different types of fluorescence probes available and the probe characteristics appropriate for the system under investigation. Several examples from the literature are discussed that illustrate different practical aspects of the technique applied to diverse systems. © 1999 Academic Press

The essence of biological specificity resides in the energetic, dynamic, and structural aspects of biomolecular interactions. Although a great deal of emphasis has been placed on elucidation of structural aspects of biomolecules (primarily through the use of X-ray diffraction studies and, more recently, NMR methodologies) our understanding of biomolecular interactions and specificities cannot proceed in the absence of knowledge on the energetics and dynamics of the systems. This article focuses on determinations of the free energy of biomolecular interactions with a particular emphasis on protein–protein interactions.

One of the most important attributes of proteins is their ability to interact, with varying degrees of affinity and specificity, with other proteins. In some cases, the interacting proteins may be identical, such as with oligomeric proteins composed of like subunits. Oligomeric proteins containing multiple and identical, distinct polypeptides chains are common and many examples of dimers, trimers, tetramers, hexamers, and even higher aggregates are well known. Oligomeric proteins containing multiple, nonidentical subunits are also known, ranging from simple heterodimers to large protein complexes such as ribosomes.

The strength of a particular protein–protein interaction depends on the free energy change associated with complex formation. This free energy change, ΔG, can in principle be understood in terms of the enthalpy and entropy associated with complex formation ($\Delta G = \Delta H - T\Delta S$). Measurements of the dissociation constant of the complex (e.g., dimer-to-monomer dissociation) will yield the free energy change according to the relation $\Delta G = -RT \ln K_D$, where R is the universal gas constant, T the absolute temperature, and K_D the dissociation constant. The strengths of protein interactions are known to vary according to the physiological function involved. For example, protein–receptor interactions are often quite strong (K_D values in the range of nanomolar or less) due to the necessity to bind certain proteins that are present only at low circulating concentrations. Protein complexes that are more transient, such as those formed between some tricarboxylic acid cycle enzymes (see below), may have K_D values greater than 10 μM. The aggregation state of some multimeric enzymes may also provide a means of regulating the enzymatic activity of the system. Many oligomeric proteins bind small molecules (ligands) with varying affinities. In some cases, the binding of the ligand (which may be bound to the protein either noncovalently or covalently) may influence the free energy of the protein–protein interaction. In the terminology of Weber (1, 2), the macroassociation constants (protein–protein association) may be coupled to the microassociation constants (ligand binding). Hemoglobin provides a well-known example of this phenomenon as the free energy of association for the dimer-to-

[1] To whom correspondence should be addressed. E-mail: djameson@hawaii.edu.

1046-2023/99 $30.00

tetramer equilibria (at 21.5°C) of fully oxygenated human hemoglobin is -8.09 kcal M^{-1} while the corresponding free energy for unliganded hemoglobin is -14.35 kcal M^{-1} (3). It is thus evident that a complete appreciation of the molecular basis of protein function requires quantitative knowledge of the free energies associated with the possible interactions.

The methods used to study the dissociation of oligomeric proteins may be classified according to whether the dissociation is *spontaneous* or *induced*. Spontaneous dissociation avoids the introduction of external free energy perturbations such as those due to changes in temperature, pressure, or additional ligands (such as urea and guanidinium chloride) and can be achieved by dilution of the protein solutions to an extent that permits the appearance of measurable dissociation. To obtain reliable data it is usually necessary to examine the dissociation in the range of approximately 10 to 90% which invokes observations at concentrations in the range of 10 times to 1/10th of the dissociation constants (see below). Complexes most amenable to the study of their spontaneous dissociation are those with dissociation constants in the micro- to nanomolar range. In spontaneous dissociation, the increase in the degree of dissociation results from the decrease in the rate of association (which is a bimolecular reaction) brought about by dilution, while the rate of dissociation (which is a unimolecular reaction) is constant. In induced dissociation the interpretation of the data is more delicate since changes in the chemical potentials of oligomers and monomers may occur independently of the changes that follow the spontaneous dissociation as the result of first order effects on the subunits' conformations by the effects of pressure, temperature, or added ligands.

Direct measurements of the average mass or volume of the particles can be translated into the degree of dissociation of the aggregates with a minimum of assumptions as to the stoichiometry involved. The methods of measurement should be applicable at the low concentrations at which thermodynamic behavior is ideal, and two methods have been found to be particularly useful, namely, light scattering and fluorescence polarization. Changes in Rayleigh scattering are generally confined to the study of equilibria of particles on the order of 1 MDa that disaggregate into much smaller subunits. This method has found good application to the virus capsids, multimeric proteins such as hemocyanin and erythrocruorin, and indefinitely aggregating systems like actin, myosin, and tubulin. However, scattering differences are virtually inapplicable to the dissociation of smaller dimers, trimers, or tetramers. In these cases the variations in scattering intensity that follow on changes in the particle associations are small and can be completely obliterated by unspecific aggregation of a small fraction (1% or less) of the total protein into large, strongly scattering aggregates. Fluorescence spectroscopy, on the other hand, is particularly well suited for studies on protein–protein interactions. This suitability derives in part from the inherent sensitivity of the technique which, in favorable cases, permits quantitation of fluorophores at subnanomolar levels and, in exceptional circumstances, at the level of a few molecules. Additionally, the characteristic time scale of the emission process, in the range of nanoseconds to tens of nanoseconds, allows determination of the rotational hydrodynamics of macromolecules in the range of ten to hundreds of kilodaltons. The method also permits rapid and facile alterations in the solvent milieu under equilibrium conditions, i.e., in the absence of physical separation of the interacting systems and in the absence (unless desired) of external forces such as the elevated pressure generated in ultracentrifugation. Unlike Rayleigh scattering, steady-state fluorescence polarization weighs the components according to the fraction of the total emitted fluorescence they represent, and is therefore not seriously affected by the presence of a small fraction of the total as high-molecular-weight aggregates.

The study of the stability of aggregates by determination of the degree of dissociation requires examination of solutions at concentrations within one order of magnitude of the constant of the dissociation of the aggregate into smaller particles. From present experience, the smaller protein aggregates have characteristic concentrations, $C_{1/2}$, at which they are half-dissociated, of 10^{-6} to 10^{-12} M (1). Fluorescence observations can be comfortably made at micro- to nanomolar concentrations, but become more difficult at lower concentrations. This limitation is considerable when one attempts to study equilibria with $C_{1/2}$ below 10^{-10} M, not only because of the decline in the signal-to-noise ratio and the presence of fluorescent contaminants in amounts comparable to or greater than the signal, but also because at these low concentrations the surface of the containing vessel becomes comparable to the total cross section of the dissolved protein. Any differential adsorption of the components onto the vessel walls can thus introduce large errors in the characterization of the dissociation equilibrium. These considerations are not meant to discourage the use of this method, but rather to point out that appropriate caution must be applied as the dissociation constants being elucidated become smaller.

Ideally, one should like to observe the system throughout a concentration range such that the system passes from 10% dissociated to 90% dissociated, a range referred to as the span of the dissociation (1). Consider the case of a dimer that can dissociate into two monomers,

$$[\mathrm{D}] \leftrightharpoons 2[\mathrm{M}], \qquad [1]$$

where [D] and [M] are the equilibrium concentrations of dimer and monomer, respectively. The dissociation constant for this process is thus

$$K_D = \frac{[M]^2}{[D]}. \quad [2]$$

The dissociation constant can also be related to α, the degree of dissociation (i.e., α equals unity for complete dissociation and zero for complete association), by

$$K_D = \frac{4\alpha^2 C}{(1-\alpha)}, \quad [3]$$

where C represents the total protein concentration (in terms of the dimer). This equation can then be rearranged and put in logarithmic form to yield

$$\log \frac{K_D}{4C} = \log\left[\frac{\alpha^2}{(1-\alpha)}\right]. \quad [4]$$

A plot of α versus log C represents the dissociation curve of the system and the concentration at which $\alpha = 0.5$ corresponds to the dissociation constant. One can readily verify that the span of this curve, i.e., the concentration range over which α changes from 0.1 to 0.9, is 2.86 decimal log units[2] or 729-fold (1). The principles outlined in this article may also be applied to the study of higher-order aggregates, such as tetramers. In these cases, however, the interpretation of the results may be less straightforward due to the presence of multiple species of varying size. Tetramer dissociation into monomers, for example, would be expected to proceed via dimer intermediates but observation of dimer species will require that the dissociation constant for the dimer-to-monomer equilibrium is distinctly *lower* than the tetramer-to-dimer dissociation constant. The resolution of three distinct rotating species using steady-state polarization data requires a careful choice of probe characteristics (e.g., lifetime), very high precision data, and well-separated dissociation constants spread out over an accessible concentration range. If the dimer-to-monomer dissociation constant is higher than the tetramer-to-dimer dissociation constant, then dissociation of the tetramer will be immediately followed by dimer dissociation. In the case of tetramer-to-monomer dissociation, the log span of the dissociation curve will be 1.59.

[2] Xu and Weber (4) first drew attention to a dimer-to-monomer dissociation curve with a span less than 2.86 log units and proposed that this reduction of the span results from a time-dependent loss of affinity that occurs when the monomer interfaces in the dimer become separated from each other and adopt, on contact with the solvent, conformations that differ from those present in the dimer previous to dissociation. At each degree of dissociation these conformational differences reach a stationary condition depending on the lifetime of the free monomer, which provides the opportunity for *conformational drift,* and the lifetime of the dimer during which the drift is partially or totally repaired. In more recent years other dimers, including the ARC protein (5) and a mutant of *Rhodobacter rubisco* (6), have also shown dilution curves with reduced logarithmic span. In fact, the observation of a shortened logarithmic span in dissociating dimers seems to be just as common as that of a normal logarithmic span.

FLUORESCENCE POLARIZATION

The systematic application of fluorescence methodologies, including fluorescence polarization, to biochemistry began with the pioneering work of Gregorio Weber (7). An excellent treatment of the origins of the polarization of fluorescence has been given by Weber (8); our treatment here will not enter into the same rigorous detail and readers with a sustaining interest

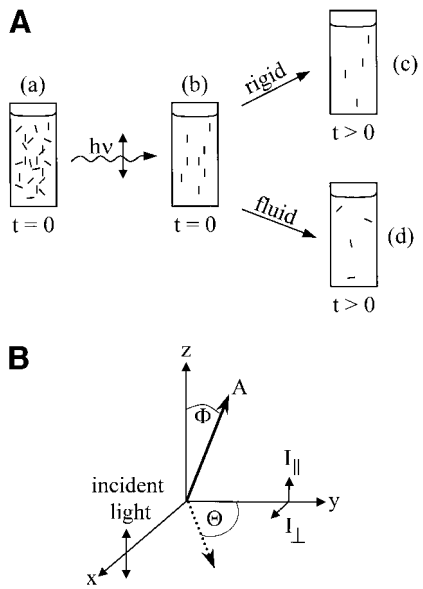

FIG. 1. (A) Schematic overview of photoselection and excited-state processes involved in fluorescence polarization. Cuvette a contains fluorophores in their ground state; the direction of the lines indicates the orientations of their absorption dipole moments. Cuvette b depicts the system after absorption of the incident exciting light; fluorophores with their absorption dipoles roughly aligned with the direction of the electric vector of the incident light are preferentially excited. Cuvette c depicts the system at a short time after excitation under the condition that the medium is sufficiently rigid to prevent rotational diffusion of the excited fluorophores; also indicated is the fact that some excited states have been deactivated. Cuvette d depicts the system at a short time after excitation under the condition that the medium is sufficiently fluid to permit rotational diffusion of the excited fluorophores. (B) Diagram depicting the relative orientations of the electric vector of the excitation that is polarized in the XZ plane, the absorption dipole (A) where the angle ϕ is in the ZY plane, the projection of A on the XY plane (the angle Θ is in the XY plane), and observation along the Y axis through polarizers oriented either parallel to the Z axis ($I_\parallel$) or the X axis ($I_\perp$).

are referred to that article. We shall, however, give a brief overview [for more detailed discussions see also (9–11)]. In fluorescence spectroscopy, the signal is generated by illumination of the sample by monochromatic light at a wavelength absorbed by the probe molecule. The energy of the absorbed light raises the probe molecule to an excited electronic energy level which typically persists for a time in the range of nanoseconds to tens of nanoseconds until the molecule reverts to the ground state with the emission of a photon. If the exciting light is polarized, i.e., if its electric vector is characterized by a unique direction with respect to the laboratory axis, then a photoselection process occurs on illumination and only probe molecules with their absorption dipoles suitably oriented (i.e., approximately parallel to the electric vector of the exciting light) are excited (Fig. 1A). More precisely, the probability that a molecule will absorb an incident photon is proportional to the orientation between the transition dipole moment of the molecule and the direction of the electric vector of the exciting light (Fig. 1B). If the excited-state dipole moment (the emission dipole) is oriented parallel to the absorption dipole moment and if no change in the orientation of the probe occurs between the excitation and emission processes, then the emitted light will also be polarized. For a solution of immobile and randomly oriented absorption dipoles the maximum polarization will be $+\frac{1}{2}$. If, however, the probe rotates during the excited-state lifetime, then the emitted light will be depolarized relative to the exciting light and the extent of depolarization can provide information on the rotational diffusion process. These processes are depicted in Fig. 1. Polarization is defined as

$$P = \frac{I_{\parallel} - I_{\perp}}{I_{\parallel} + I_{\perp}}, \qquad [5]$$

where P is the observed polarization, $I_{\parallel}$ is the intensity of the parallel component (i.e., parallel to the vertical laboratory axis), and $I_{\perp}$ is the intensity of the perpendicular component. Fluorescence anisotropy (r), on the other hand, is defined as

$$r = \frac{I_{\parallel} - I_{\perp}}{I_{\parallel} + 2I_{\perp}}. \qquad [6]$$

One can show that

$$r = \frac{2}{3}\left(\frac{1}{P} - \frac{1}{3}\right)^{-1} \qquad [7]$$

and

$$r = \frac{2P}{(3 - P)}. \qquad [8]$$

The use of polarization/anisotropy to elucidate binding isotherms arose from the observations of Weber (12) on the additivity properties of polarization. Specifically, he demonstrated that (for polarized excitation)

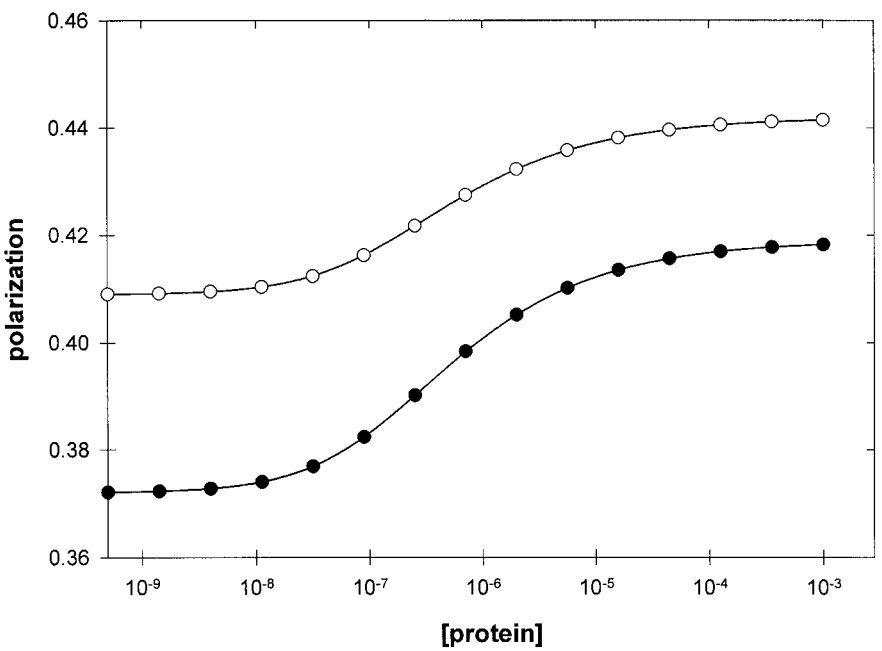

FIG. 2. Simulations of the concentration-dependent changes in polarization associated with either a 60-kDa dimer (●) dissociating into 30-kDa monomers or a 100-kDa dimer (○) dissociating into 50-kDa monomers. In both cases the proteins are labeled with a 4-ns probe that does not experience local mobility. The dissociation constant in both cases is 10^{-6} M.

$$\left(\frac{1}{P_{obs}} - \frac{1}{3}\right)^{-1} = \sum f_i \left(\frac{1}{P_i} - \frac{1}{3}\right)^{-1}, \quad [9]$$

where P_{obs} is the actual polarization observed arising from i components, where f_i represents the fractional contribution of the ith component to the total emission intensity. This additivity aspect can be expressed in terms of anisotropies as

$$r_{obs} = \sum f_i r_i. \quad [10]$$

We should note, however, that anisotropy and polarization have the same information content and the use of one or the other term is a matter of convenience, not of substance.

We note the f_i term represents fractional contribution of the ith species to the *photocurrent* detected. If the quantum yields of the various fluorescing species differ, or if the emitting species fluoresce at different wavelengths and the measurement is being done with filters or a monochromator that favors one wavelength over another, then one must weigh the ith species accordingly to convert the data to the molar quantities required for correct assignment of the dissociation curve. In the case of two species, dimer and monomer, with differing quantum yields, Eq. (10) takes the form (13)

$$r_{obs} = \frac{r_D I_D + r_M I_M}{I_D + I_M}, \quad [11]$$

where I_D and I_M are the intensities of the dimer and monomer species, respectively, recorded by the photodetector. Since these intensities will be proportional to the quantum yields of the monomers and dimers, respectively, Q_M and Q_D, one can write

$$I_M = Q_M \alpha, \quad I_D = Q_D(1 - \alpha), \quad [12]$$

or

$$\alpha = \left[1 + Q\left(\frac{r_{obs} - r_M}{r_D - r_{obs}}\right)\right]^{-1}, \quad [13]$$

where $Q = Q_D/Q_M$.

The relationships between polarization, fluorescence lifetime, and rotational diffusion of spherical particles were explored by Perrin (14) and later extended to nonspherical particles by Weber (12). The Perrin–Weber equation states

$$\left(\frac{1}{P} - \frac{1}{3}\right) = \left(\frac{1}{P_0} - \frac{1}{3}\right)\left(1 + \frac{3\tau}{\rho}\right), \quad [14]$$

where P is the observed steady-state polarization, P_0 is the limiting or intrinsic polarization in the absence of depolarizing influences such as rotation and energy

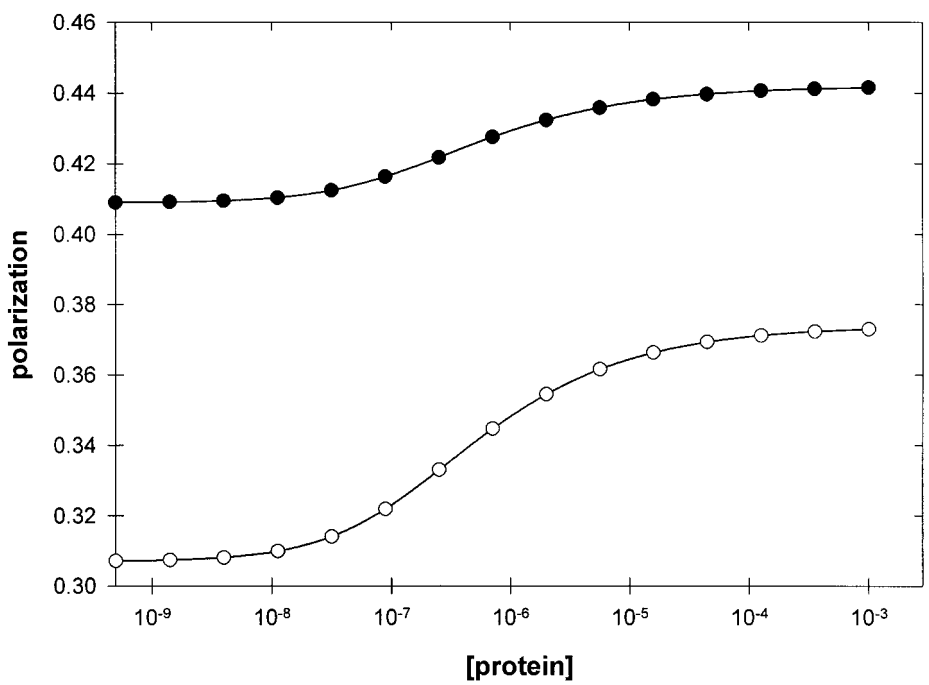

FIG. 3. Simulations of the concentration-dependent change in polarization associated with a 100-kDa dimer, labeled with either a 4-ns (●) or 13-ns (○) probe that does not experience local mobility, dissociating into 50-kDa monomers. The dissociation constant is 10^{-6} M.

transfer,[3] τ is the excited-state lifetime (which corresponds to the time after excitation at which the number of excited molecules has been reduced to $1/e$ of its original number), and ρ_h is the harmonic mean of the Debye rotational relaxation times about the principal axes of rotation. ρ_h is defined as

$$\rho_h^{-1} = \frac{(\rho_1^{-1} + \rho_2^{-1} + \rho_3^{-1})}{3}, \quad [15]$$

where ρ_1, ρ_2, and ρ_3 are the rotational relaxation times about the three principal rotation axes. For a spherical molecule $\rho_1 = \rho_2 = \rho_3 = \rho_0$ and

$$\rho_0 = \frac{3\eta V}{RT}, \quad [16]$$

where η is the medium's viscosity, V the molar volume monitored by the probe, R the gas constant, and T the absolute temperature. It follows that

$$\rho_0 = \frac{3\eta M(v + h)}{RT}, \quad [17]$$

where v is the partial specific volume and h the degree of hydration. We should also note that it is not uncommon to see the term "rotational correlation time," often denoted as τ_c, used in place of the rotational relaxation time. The information content of these terms is similar since $\rho = 3\tau_c$ but we have observed that some people become rather fervently attached to the use of one term or the other. As was pointed out in a recent review (15), in the original development of rotational motions of fluorophores the *rotational relaxation time* was used and only later, during the development of nuclear magnetic resonance, was the term *rotational correlation time* used. It thus seems appropriate for fluorescence practitioners to use ρ, but certainly the adoption of one or the other term should not cause confusion.

For the case of a rigid, spherical protein monomer of molecular weight 30 kDa, in aqueous buffer at 20°C (η = 0.01 P), assuming a partial specific volume of 0.74 ml/mg [note that the partial specific volume may be calculated from the amino acid sequence using the method of Cohn and Edsall (16)] and a hydration of 0.2 ml/g and using the gas constant of 8.31×10^7 erg mol^{-1} K^{-1}, the Debye rotational relaxation time calculated from Eq. [17] is

$$\rho = \frac{3(0.01)(30000)(0.74 + 0.2)}{(8.31 \times 10^7)(293)},$$

which gives ρ = ~35 ns. If we assume that the rotational relaxation time of the dimer is then 70 ns (which of course assumes, a bit unrealistically, that the two spherical monomers form a spherical dimer), and apply the Perrin–Weber equation for the case of a probe with a 4-ns lifetime and a P_0 of 0.48 (such as fluorescein excited near 490 nm), then we find that the dimer-to-monomer dissociation will give a change in polarization from 0.419 to 0.372, i.e., a polarization change of 0.047. Given that the precision of polarization measurements is generally in the range of 0.002 or better, the dimer-to-monomer dissociation can easily be followed in this case. If the monomers are larger though, for example, 50 kDa, then the calculated rotational relaxation times for dimer and monomer are ~58 and 116 ns, which give polarizations of 0.409 and 0.442, respectively. This polarization change of 0.033 would be slightly more difficult to resolve than the previous case due to the smaller change in polarization, which in turn is due to the decreased ratio of the lifetime to the rotational relaxation time (τ/ρ). Simulations of the polarization-versus-protein concentration curves for these two cases, i.e., the 30- and 50-kDa monomers, with 4-ns probes and dissociation constants of 10^{-6} M, are shown in Fig. 2. If the lifetime of the probe is increased to 13 ns (a typical value for many naphthalene-based probes such as 1,5 dansyl and IAEDANS; the 2,5-dansyl derivative, on the other hand, has a longer lifetime in the range of 25 ns) then the polarization values associated with the 100 kDa- to 50-kDa dissociation case (assuming still P_0 = 0.48, i.e., excitation above 360 nm) become 0.374 and 0.307, a change of 0.067, i.e., about twice the change expected for the fluorescein probe. Simulations of polarization-versus-protein concentration curves for this case, i.e., 50-kDa monomers with either fluorescein (4 ns) or dansyl (13 ns) probes and dissociation constants of 10^{-6} M, are shown in Fig. 3. At first glance it would thus

[3] The value of P_0 is determined by the angle (ϕ) between the absorption oscillator and the emission oscillator. For a population of randomly oriented fluorophores this value can, in principle, range between $+\frac{1}{2}$ and $-\frac{1}{3}$, its magnitude being given by the expression

$$\left(\frac{1}{P_0} - \frac{1}{3}\right) = \frac{5}{3}\left(\frac{2}{3\cos^2\phi - 1}\right).$$

The positive limit, 0.5 (or 0.4 for anisotropy), which occurs when absorption and emission dipoles are colinear, i.e., $\phi = 0°$, is often assumed and in fact was a reasonable approximation in the days when only a few fluorophores based on naphthalene and fluorescein were used along with arc lamps/monochromator systems for excitation, which allowed excitation well into the final absorption band. Given the immense proliferation of commercially available probes and the increasing use of lasers with various fixed outputs (such as 325 nm for helium–cadmium lasers), the fluorescence practitioner would do well to verify the P_0 value for the probe of choice given the particular excitation and emission wavelengths used. Pyrene, for example, exhibits a P_0 that is generally low (<0.2) and varies with both excitation and emission wavelength. Tryptophan also demonstrates a complex excitation polarization spectrum and the highest P_0 value (0.4) is not attained below excitation wavelengths of 300 nm.

seem that the increased polarization change observed with the longer-lifetime probe favors its use over the shorter-lifetime probe. Matters are not always that simple, however, since the short-lifetime probe in this case, fluorescein, has a much larger extinction coefficient than typical naphthalene-based probes (~70,000 $cm^{-1}\ M^{-1}$ compared with ~5500 $cm^{-1}\ M^{-1}$) and usually a higher quantum yield as well. Moreover, longer excitation wavelengths almost always result in lower background signal. Hence, fluorescein can be used at significantly lower concentrations than naphthalene probes; for example, fluorescein polarizations have been measured at 10^{-13} M (17) while naphthalene probes are difficult to use below nanomolar concentrations and intrinsic tryptophan fluorescence presents problems below about 10^{-8} M.

As discussed earlier, plots of polarization (or anisotropy) versus protein concentration may be replotted in terms of α, the degree of dissociation versus concentration [Eq. (4)] as shown in Fig. 4. Both cases shown in Fig. 3, i.e., the 4- and 13-ns probes, give identical curves when plotted in terms of the degree of dissociation. Simulations are also shown in Fig. 4 for dimers with dissociation constants of 10^{-4} and 10^{-8} M.

In practice, the polarizations observed for cases such as those described above are almost always lower than those calculated using Eqs. [14] and [17]. This difference is usually due to the presence of local probe motion by the covalently tethered probe (although depolarization due to fluorescence resonance energy transfer may also occur as discussed below for the case of ribosomal protein L7/L12). Local probe motions were originally described by Wahl and Weber (18) in their studies on dansyl-labeled IgG antibodies and were ascribed to mobility of the probes about their points of attachment. As our knowledge of protein dynamics and structures has improved, we now appreciate that "local" motion may include mobility of larger regions or domains of the protein. In some cases, especially in the case of tryptophan residues buried at subunit interfaces, the local probe mobility may be increased significantly on protein dissociation, thus increasing the difference in polarization between the associated and dissociated states. The additional depolarization caused by local probe mobility may be approximated by the addition of a "Soleillet" term (8) to Eq. 14, namely,

$$\left(\frac{1}{P}-\frac{1}{3}\right)=\left(\frac{1}{P_0}-\frac{1}{3}\right)\left(\frac{2}{3\cos^2\omega-1}\right)\left(1+\frac{3\tau}{\rho}\right), \quad [18]$$

where ω represents the angle associated with the local motion. Angles of 10° to 30° have been typically observed for tyrosine and tryptophan motions in protein. The effect of an increase in local probe mobility on protein dissociation can thus be considerable. Figure 5 shows simulations for the case of the 100-kDa dimer with a fluorescein (4 ns) probe and a dissociation constant of 10^{-6} M in which the probe has no local mobility in the dimer state and increases of 0°, 10°, 20°, and 30° on dissociation into monomers.

In other cases, if the extent of probe mobility is very extensive in both monomer and dimer, the dissociation

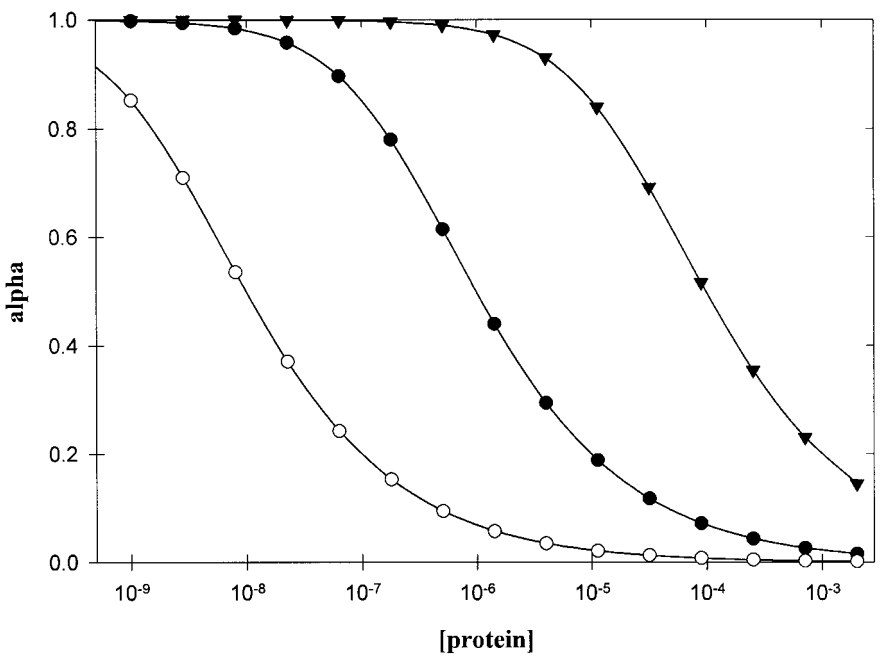

FIG. 4. Replot of the polarization (for both the 4- and 13-ns data) versus concentration data shown in Fig. 3 in terms of α, the degree of dissociation, calculated from the polarization data ($K_D = 10^{-6}$). Note that both curves from Fig. 3 coincide when replotted as the α function (●). Also shown are simulations for dissociation constants of 10^{-4} M (▼) and 10^{-8} M (○).

may be difficult to detect since there may be very little change in the overall polarization as the state of protein aggregation changes (this situation occurs in the case of L7/L12 discussed below). In the case of noncovalently associated probes, such as NADH, FAD, and porphyrins, there is typically very little local probe mobility, since noncovalent associations of reasonable strength usually require multiple interactions of amino acid residues with the fluorophore which act to restrict its mobility; examples of such limited probe mobilities can be found, for the cases of NADH associated with a dehydrogenase enzyme (19) and porphyrin associated with horseradish peroxidase (20).

Another consideration that may cause deviation of the observed polarization from that calculated from Eq. [16] or [17] is the shape of the protein complex. As mentioned earlier, the rotational relaxation time used in the Perrin–Weber equation (Eq. [14]) represents the harmonic mean of the rotational relaxation times about the principal axes of rotation. Many proteins and protein complexes, however, are nonspherical and, in principle, careful determinations of the polarizations of fluorophores associated with such systems can provide information on the shape of the protein or protein complex. In fact, this consideration was one of the original motivations for Gregorio Weber's pioneering studies on dansyl-labeled proteins (12) since, at that time, structural information on proteins was limited to hydrodynamic studies. In these studies, Weber considered explicitly both oblate (disk-shaped) and prolate (cigar-shaped) ellipsoids of revolution and the influence of the ratio of the major and minor axes on the rotational diffusion of the molecule. Simulations of the effects of protein shape on the observed polarizations are given in Table 1 for the case of the a 100-kDa dimer labeled with dansyl (13 ns). The various cases considered are those corresponding to spherical monomers and dimers and intrinsically oblate ($a/b = 2$ or 5) or prolate ($a/b = 2$ or 5) monomers that associate in an end-to-end manner. This table is intended simply to provide a rough estimate of the effect of shape on the observed polarization.

One example of the application of these considerations to evaluate fluorescence polarization data and compare them with other hydrodynamic data obtained using intrinsic viscosity and ultracentrifugation studies is provided by Rholam and Nicolas (21), who studied dansylated neurophysin and concluded that the axial ratios of the monomers and dimers were 5.2 and 3.5, respectively. Moreover, these data in combination with their other hydrodynamic results led them to conclude that the monomers associated in a side-by-side manner when forming the dimer. However, the presence of significant domain motion or probe mobility may complicate such detailed analyses in most larger protein systems. In such cases, time-resolved anisotropy data and global analysis methodologies are valuable (20).

Fluorescent protein probes may be arbitrarily divided into two categories, namely, intrinsic and extrinsic. By intrinsic we refer to molecules that are naturally associated with target biomolecules and that

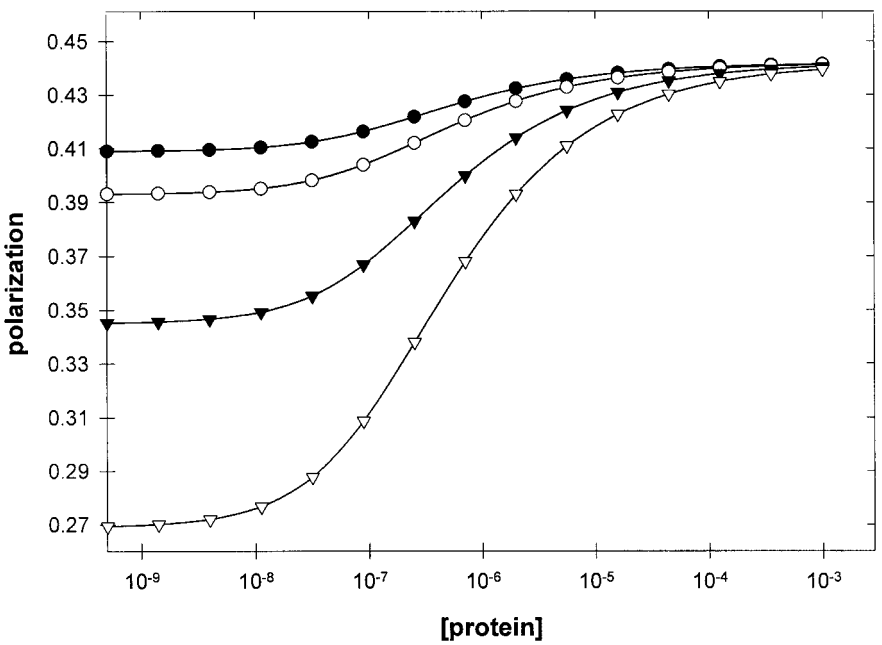

FIG. 5. Simulations of a 100-kDa dimer, labeled with a 4-ns probe, dissociating into 50-kDa monomers. The probe experiences no local mobility when bound to the dimer and varying degrees of local mobility when bound to the monomer. The associated extents of angular local mobility of the probe bound to the monomer are 0° (●), 10° (○), 20° (▼), and 30° (▽). The dissociation constant is 10^{-6} M in all cases.

possess sufficient fluorescence yields to be of practical use. In this category, we commonly consider the amino acids tyrosine and tryptophan, the coenzymes FAD and NADH, and some of the porphyrins. We note that green fluorescent protein (GFP) is also in this category. The other category, i.e., extrinsic probes, includes reagents that can be associated with a protein by either noncovalent or covalent means. Noncovalent probes include the anilinonaphthalene probes ANS and bis-ANS and quasi-natural probes such as fluorescent nucleotide analogs (22). Covalent probes include those that react with different protein functional groups. Amine-reactive probes include dansyl chloride, fluorescein isothiocyanate (FITC), and many others. Sulfhydryl reactive probes include IAEDANS, acrylodan, and various maleamide- and iodoacetamide-linked fluorophores which include fluorescein, rhodamine, and pyrene. The choice of which probe to use will clearly be dictated by the properties of the protein system under investigation. We note that the attachment of covalent probes, in a random fashion to a protein with a relatively large number of potential labeling sites, will result in a Poisson distribution of the probes among the protein population. Hence, even when the average labeling ratio (probe to protein) is low, for example less than unity, a proportion of the protein will carry multiple probes.

As regards the utility of noncovalent probes for following protein dissociation, the central consideration, besides the fluorescence characteristics of the probe, is the relative strength of the micro- and macroassociation constants. In other words, if the probe's dissociation constant is not significantly lower than the oligomer dissociation constant, then on dilution the probe will dissociate before protein dissociation occurs. This requirement is not generally met and hence noncovalent probes, while often valuable in providing information on the dynamics of the probe's environment or overall hydrodynamic aspects of the protein, are not generally applicable in protein dissociation studies. Another choice of probe may be the intrinsic protein fluorescence. Tyrosine fluorescence is relatively weak and usually masked by tryptophan emission. If the target protein has no tryptophan residues, however, it may be possible to use the tyrosine fluorescence to follow protein dissociation. Such studies are rare, however, presumably owing to the relative paucity of oligomeric proteins lacking tryptophan but also to the intrinsic lack of sensitivity associated with tyrosine due to its low extinction coefficient ($\sim$1280 cm^{-1} M^{-1} at 280 nm) and the fact that the required excitation in the deeper ultraviolet readily excites many fluorescent contaminants in buffer systems, reducing the signal to background. Tryptophan is a much more common probe of protein dynamics, especially since the advent of site-directed mutagenesis techniques which permit the construction of proteins with a single tryptophan residue positioned at selected points along the peptide chain.

TABLE 1

Effect of Shape on Polarization[a]

Monomer shape	Polarization monomer	Polarization dimer
Simple sphere (a/b = 1)	0.307	0.388
Oblate (a/b = 2)	0.349	0.412
Oblate (a/b = 5)	0.323	0.391
Prolate (a/b = 2)	0.384	0.434
Prolate (a/b = 5)	0.373	0.424

[a] 100-kDa dimers/50-kDa monomers labeled with randomly oriented dansyl probes. Calculations assume a lifetime of 13 ns, P_0 = 0.48, and no local probe mobility. In forming the dimers, the monomers are assumed to align end-to-end.

EXAMPLES

We now describe several studies from the literature to illustrate specific details of the methodologies involved, including the protein labeling procedures.

Mitochondrial Malate Dehydrogenase

Polarization measurements were used to study the dimer/monomer equilibrium of FITC-labeled mitochondrial malate dehydrogenase, a dimeric enzyme composed of identical subunits, each with 314 amino acids (23, 24). The original observations of Shore and Chakrabarti (23) on this system had indicated a dimer-to-monomer dissociation constant of $\sim 2 \times 10^{-7}$ M. A number of other studies [reviewed in (24)], however, had indicated dissociation constants for this dimer ranging from greater than 2×10^{-7} M down to subnanomolar. The results of Sanchez *et al.* (24), replotted in Fig. 6, demonstrated that the observed polarization depended on the method of protein preparation and that an FITC adduct of mitochondrial malate dehydrogenase (mMDH) with high specific activity could be prepared that would not dissociate even at nanomolar concentrations. Specifically, the mMDH was labeled using either a phosphate buffer or Tris buffer protocol. In the phosphate buffer protocol, lyophilized mMDH powder was dissolved in 0.1 M potassium phosphate buffer, pH 8.0, to a concentration between 3 and 4×10^{-5} M, and desalted, at room temperature, through a NAP-5 column (Sephadex G-25 from Pharmacia Inc.) with the same buffer. The eluted sample was incubated with a 20-fold molar excess of FITC at 4°C and allowed to react for a maximum of 4 h. Free FITC was removed by the NAP-5 column using the same buffer system. In the Tris buffer protocol, the conjugates were made using 50 mM Tris–acetate buffer at pH 8.0. Lyophilized mMDH was dissolved in buffer to a concentration of

10^{-5} M, incubated with a fivefold molar excess of FITC, and allowed to react for 24 h at 4°C. The free FITC was removed using the NAP-5 column. The fluorescein-labeled enzyme was then dialyzed at 4°C for several hours against 50 mM Tris–acetate buffer, pH 8.0. Protein concentrations were determined using the Bradford method (25) and labeling ratios of the FITC–mMDH conjugates were calculated using a molar extinction coefficient for fluorescein of ϵ_{499} = 70,000 M^{-1} cm^{-1}. In this study, time-resolved polarization measurements were also used to confirm that the rotational relaxation time of the FITC–mMDH (~103 ns) was consistent with the nonspherical shape of the dimeric protein. This study clearly demonstrates that sample preparation and buffer conditions can have profound effects on the dissociation properties of a protein, as indicated in Fig. 6.

Ribosomal Protein L7/L12

Hamman *et al.* (26, 27) studied the dynamics and dimer/monomer equilibria of L7/L12, a homodimer (each subunit is ~12 kDa) present in the 50S subunit of *Escherichia coli* ribosomes, which is essential for ribosome function in protein biosynthesis. Each L7/L12 subunit is considered to be comprised of two distinct, organized, structural domains: a helical N-terminal domain (residues 1–34) required for binding of the L7/L12 dimer to L10 in the 50S ribosomal subunit, and a globular C-terminal domain (residues 53–120), responsible for interaction with nonribosomal proteins such as elongation factor Tu. These domains are separated by a putatively disordered "hinge" region, residues 35–52. Wild-type L7/L12 has neither cysteine, tryptophan, nor tyrosine residues, and site-directed mutagenesis was used to introduce cysteine residues at various locations along the polypeptide chain. Various sulfhydryl-reactive fluorescence probes were then attached to cysteine residues located either in the C-terminal domain (residues 63, 89, and 99) or the N-terminal domain (residues 12 and 33). The results of both steady-state and time-resolved measurements demonstrated that the two C-terminal domains move freely with respect to one another and with respect to the dimeric N-terminal domain. The polarizations of these various adducts, as a function of protein concentration, are shown in Fig. 7. One notes a significant reduction in the polarization of the fluorescein probes attached to the N-terminal domain (residues 12 and 33) as the protein concentration decreases, while the respective polarization change for the fluorescein attached to the C-terminal domain (residue 89) is not as great.

One also notes that the polarizations associated with L7/L12 either singly and doubly labeled at position 33 differ significantly at concentrations at which the protein is dimeric. Specifically, when each subunit in the L7/L12 dimer has a fluorescein attached to position 33, the fluorescein moieties are in sufficient proximity to experience depolarization due to homo-energy transfer. On dissociation, the subunits become separated and homotransfer cannot occur. This phenomenon of homo-energy transfer has been used to study changes in protein aggregation states and subunit interchange among populations of protein oligomers (28, 29). Another interesting observation is the fact that L7/L12

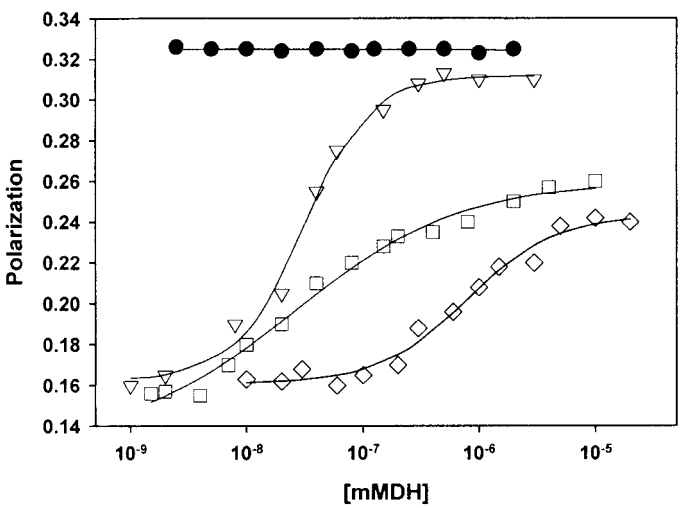

FIG. 6. Polarization as a function of protein concentration for different mMDH–FITC conjugates prepared using either a phosphate or Tris buffer labeling protocol. As shown, the conjugate prepared using the phosphate buffer protocol did not show a concentration dependent change in the polarization (●), whereas the conjugates prepared using the Tris buffer protocols (all open symbols) displayed a concentration-dependent variation of the polarization which varied for different preparations.

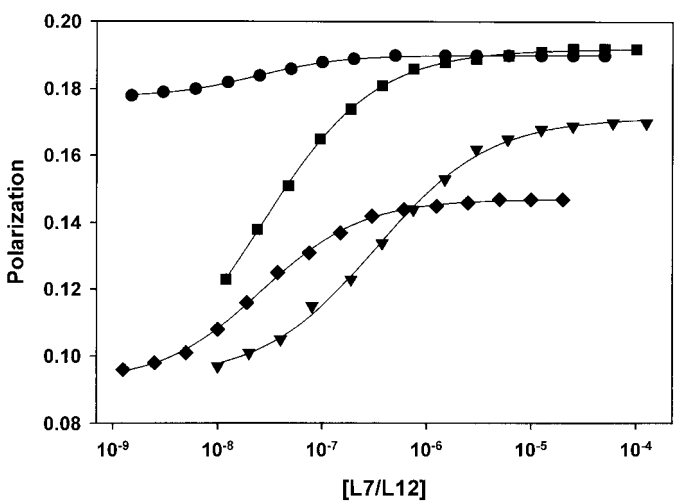

FIG. 7. Concentration dependence of the polarization of L7/L12 variants modified in the C- or N-terminal domain with fluorescein attached to cysteine residues. The curves correspond to modification of residue 89 in the C-terminal domain (●) and residues 12 (▼) and 33 (◆, doubly labeled; ■, singly labeled) in the N-terminal domain.

labeled at residue 12 exhibits a higher dissociation constant than L7/L12 labeled at position 33. This difference has been attributed to the fact that residue 12 is incorporated in an α-helix which is believed to be important for the stability of the dimer (27). The range of motional properties of a probe associated with the C-terminal domain of L7/L12 are depicted in Fig. 8.

Citrate Synthase/Malate Dehydrogenase

Tompa *et al.* (30) studied the interaction of citrate synthase with malate dehydrogenase by labeling the citrate synthase with fluorescein isothiocyanate and monitoring the increase in anisotropy of this conjugate as malate dehydrogenase was added. The labeling of the citrate synthase was accomplished by adding 0.5 mg of FITC, adsorbed to Celite, to 5 mg of the protein and incubating the reaction for 20 min at 4°C. The sample was then filtered on a Sephadex G-50 column to remove the unbound dye. The dye-to-protein ratio was calculated to be 0.35 $\pm$ 0.05 assuming an extinction coefficient of 66,000 M^{-1} cm^{-1} for bound dye. The anisotropy of the 3.5×10^{-7} M labeled citrate synthase was found to be 0.15 (which corresponds to a polarization of 0.209). On addition of unlabeled mitochondrial malate dehydrogenase, up to the level of 3×10^{-5} M, the anisotropy increased to 0.225 (which corresponds to a polarization of 0.303). Assuming that the binding stoichiometry was 1:1, a dissociation constant of 1.0 $\pm$ 0.4×10^{-6} M was calculated for the protein–protein complex. Interestingly, the labeled citrate synthase also interacted with cytoplasmic malate dehydrogenase but the affinity in this case was weaker, i.e., the dissociation constant was 1.5×10^{-5} M. The effects of various metabolites on the citrate synthase–malate dehydrogenase interaction were also assessed in this study; α-ketoglutarate and NADH were found to enhance and weaken the interaction, respectively.

Other Studies

Several additional studies will be mentioned here to point the interested reader to biological systems that may be relevant to their own research endeavors. Aloj *et al.* (31) labeled bovine thyrotropin with 1,5-dansyl chloride and used intensity and polarization changes to study its binding to the receptor embedded in thyroid plasma membranes. Kopelman *et al.* (32) used the intrinsic fluorescence of retinol to quantify the interaction between retinol-binding proteins and prealbumin. Royer *et al.* (33) studied the salt concentration dependence of the aggregation properties of calf thymus and chicken erythrocyte histones labeled with 1,5-dansyl chloride using fluorescence polarization methods. Den Blaauwen *et al.* (34) used a novel ruthenium-based probe with a lifetime of ~400 ns to label SecA (a 204-kDa homodimer component of the *E. coli* translocation complex) and characterize its interaction with SecB (a 69-kDa homotetrameric molecular chaperone). In this study, both steady-state and time-resolved fluorescence anisotropy were used along with dynamic light scattering. The anisotropy titration of the labeled SecA with SecB indicated a dissociation constant of 1.6 μM.

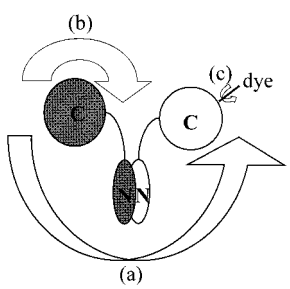

FIG. 8. Schematic diagram depicting the rotational modalities present in L7/L12 labeled in the C-terminal domain: for clarity only one cysteine-linked fluorophore is indicated. (a) Global tumbling of the entire protein. (b) Movement of the C-terminal domains with respect to one another and with respect to the N-terminal domain. (c) Local rotation of the fluorescent probe about its point of attachment.

CONCLUSION

Quantitative information on the strength of protein–protein interactions can clearly be obtained using fluorescence polarization methodologies. The successful application of the technique depends on the choice of the fluorescence probe. In particular, the photophysical characteristics of the probe, such as the excited-state lifetime, the quantum yield, and the absorption and emission maxima, as well as the probe–protein linkage chemistry, will impact on this choice. The optimum probe characteristics depend on the size of the protein complexes involved, the dissociation constant of the system, and the effects of different probe conjugation strategies on protein function. To summarize, the advantages of rapid and quantitative determinations under equilibrium conditions, the ability of the method to allow facile alterations in the solvent milieu, the attendant information on dynamic aspects of the protein system, and the relatively inexpensive instrumentation required combine to make fluorescence polarization an attractive method for characterizing protein–protein interactions.

ACKNOWLEDGMENTS

The authors thank Dr. Michael Helms for helpful discussion and assistance with some figures. D.M.J. acknowledges the support of National Science Foundation Grant MCB-9808427 and Grant-in-Aid 9950020N from the American Heart Association.

REFERENCES

1. Weber, G. (1992) Protein Interactions, Chapman & Hall, New York/London.
2. Weber, G. (1975) *Adv. Prot. Chem.* **29,** 1–83.
3. Ip, S. H. C., and Ackers, G. (1976) *J. Biol. Chem.* **252,** 82–87.
4. Xu, G.-J., and Weber, G. (1982) *Proc. Natl. Acad. Sci. USA* **79,** 5268–5271.
5. Silva, J. L., Silveira, C. F., Correia, A. Jr., and Pontes, L. (1992) *J. Mol. Biol.* **223,** 545–555.
6. Erijman, L., Lorimar, G. H., and Weber, G. (1993) *Biochemistry* **32,** 5187–5195.
7. Jameson, D. M. (1998) *Biophys. J.* **75,** 419–412.
8. Weber, G. (1966) *in* Fluorescence and Phosphorescence Analysis (Hercules, D. M., Ed.), p. 217, Wiley, New York.
9. Lakowicz, J. R. (1983) Principles of Fluorescence, Plenum, New York.
10. Jameson, D. M. (1984) *in* Fluorescein Hapten: An Immunological Probe (Voss, E., Jr., Ed.), p. 23, CRC Press, Boca Raton, FL.
11. Jiskoot, W., Hlady, V., Naleway, J. J., and Herron, J. N. (1995) *in* Physical Methods to Characterize Pharmaceutical Proteins (Herron, J. N., Jiskoot, W., and Crommelin, D. J. A., Eds.) pp. 1–63, Plenum, New York.
12. Weber, G. (1952) *Biochem. J.* **51,** 145–155.
13. Paladini, A. A., Jr., and Weber, G. (1981) *Biochemistry* **20,** 2587–2593.
14. Perrin, F. (1926) *J. Phys. Radium* **7,** 390.
15. Jameson, D. M., and Sawyer, W. H. (1995) *Methods Enzymol.* **246,** 283–300.
16. Cohn, E. J., and Edsall, J. T. (1943) Proteins, Amino Acids and Peptides, Hafner, New York.
17. Jameson, D. M., Weber, G., Spencer, R. D., and Mitchell, G. (1978) *Rev. Sci. Instrum.* **49,** 510–514.
18. Wahl, P., and Weber, G. (1967) *J. Mol. Biol.* **30,** 371–382.
19. Jameson, D. M., Thomas, V., and Zhou, D-M. (1989) *Biochim. Biophys. Acta* **994,** 187–190.
20. Brunet, J. E., Vargas, V., Gratton, E., and Jameson, D. M. (1994) *Biophys. J.* **66,** 446–453.
21. Rholam, M., and Nicolas, P. (1981) *Biochemistry* **20,** 5837–5843.
22. Jameson, D. M., and Eccleston, E. F. (1997) *Methods Enzymol.* **278,** 363–390.
23. Shore, J. D., and Chakrabarti, S. K. (1976) *Biochemistry* **15,** 875–879.
24. Sanchez, S. A., Hazlett, T. L., Brunet, J. E., and Jameson, D. M. (1998) *Protein Sci.* **7,** 2184–2189.
25. Bradford, M. M. (1976) *Anal. Biochem.* **72,** 248–254.
26. Hamman, B. D., Oleinikov, A. V., Jokhadze, G. G., Traut, R. R., and Jameson, D. M. (1996) *Biochemistry* **35,** 16672–16679.
27. Hamman, B. D., Oleinikov, A. V., Jokhadze, G. G., Traut, R. R., and Jameson, D. M. (1996) *Biochemistry* **35,** 16680–16686.
28. Erijman, L., and Weber, G. (1991) *Biochemistry* **30,** 1595–1599.
29. Erijman, L., and Weber, G. (1993) *Photochem. Photobiol.* **57,** 411–415.
30. Tompa, P., Batke, J., Ovadi, J., Welch, G. R., and Srere, P. A. (1987) *J. Biol. Chem.* **262,** 6089–6092.
31. Aloj, S. M., Lee, G., Consiglio, E., Formisano, S., Minton, A. P., and Kohn, L. D. (1978) *J. Biol. Chem.* **254,** 9030–9038.
32. Kopelman, M., Cogan, U., Mokady, S., and Shinitzky, M. (1976) *Biochim. Biophys. Acta* **439,** 449–460.
33. Royer, C. A., Rusch, R. M., and Scarlatta, S. F. (1989) *Biochemistry* **28,** 6631–6637.
34. Den Blaauwen, T., Terpetschnig, E., Lakowicz, J. R., and Driessen, A. J. M. (1997) *FEBS Lett.* **416,** 35–38.